Pentagonal multi-shell Cu nanowires

2002 J. Phys.: Condens. Matter 14 2629

(http://iopscience.iop.org/0953-8984/14/10/313)

INSTITUTE OF PHYSICS PUBLISHING JOURNAL OF PHYSICS: CONDENSED MATTER

J. Phys.: Condens. Matter **14** (2002) 2629–2636 PII: S0953-8984(02)31970-2

Pentagonal multi-shell Cu nanowires

Jeong Won Kang and Ho Jung Hwang

Semiconductor Process and Device Laboratory, Department of Electronic Engineering, Chung-Ang University, 221 HukSuk-Dong, DongJak-Ku, Seoul 156-756, Korea

E-mail: gardenriver@korea.com

Received 18 December 2001
Published 18 March 2002
Online at stacks.iop.org/JPhysCM/14/2629

Abstract

We have investigated pentagonal multi-shell-type Cu nanowires using classical molecular dynamics simulations. Each pentagonal multi-shell-type nanowire is composed of a central atomic strand and pentangular tubes made of five-times-folded {100} sheets. Their structural properties are similar to those of face-centred-cubic structures, as each of the subunits has a quadrangular-pyramid shape oriented in the ⟨100⟩ direction. Our simulations show that, at room temperature, ultrathin pentagonal Cu nanowires are seldom found; however, pentagonal multi-shell-type Cu nanowires, with diameters of several nanometres, are found in the stable structures.

(Some figures in this article are in colour only in the electronic version)

1. Introduction

In studies of nanoelectronic device fabrication, the structural properties of metallic nanowires (NWs) have been extensively investigated over the past decade. The structure of ultrathin metallic NWs has been investigated using molecular dynamics (MD) simulations, or a polygonal model. Ultrathin NWs of Au [1–6], Cu [6–9], Pb and Al [10–12], Pt and Ag [13], and Ti [14] have been investigated using MD simulations. These studies showed that helical, multi-shelled, and filled structures exist for ultrathin NWs of several face-centred-cubic (fcc) metals. Yanson *et al* [15] studied multi-shell-structured NWs of Na. The stability of Na NWs was studied by modelling them as infinite uniform jellium cylinders, and solving for the electronic structures by a self-consistent method [16]. Multi-shell NWs have also been found for several inorganic layered materials, such as WS_2, MoS_2, and $NiCl_2$ [17–19]. In recent work on metallic NWs, long metallic NWs with well-defined structures, several nanometres in diameter, have been fabricated using different methods [20–25]. Novel helical multi-shell structures have also been observed in ultrathin Au NWs [20–23].

In previous work, atomistic simulations under various conditions have produced many different polygonal Cu NWs [9], such as rectangular, pentagonal, and hexagonal ones. A free-standing pentagonal Cu NW [26] has also been found. From electron diffraction,

high-resolution transmission electron microscopy (HRTEM), and power spectra (PS) results, Lisiecki *et al* [24] have shown that a decahedron model can explain the structure of pentagonal Cu nanorods. The Cu nanorod samples were prepared by reduction of $Cu(AOT)_2$, in $Cu(AOT)_2$–iso-octane–NaCl–water colloidal self-assemblies. Many studies on the structure of nanoclusters or NWs have shown that some nanoparticles are related to a decahedron model, e.g., in Ag [27], Ni [27], Au [27–30], Cu [31, 32], and Na [33]. However, until now, the structural properties of pentagonal NWs have not been investigated.

Thiolate ligands, which produce colloidal solutions, have been used to fabricate Au nanoparticles [34–38]. These passivated clusters are relatively stable, and can be easily observed experimentally. These techniques using ligands can also be used to create passivated NWs that may have great technological importance in the fabrication of nanoscale devices. However, before the study of passivated NWs, one must investigate the properties of the bare NWs. Copper is an important engineering material, so in this investigation we present the structures and properties of ultrathin pentagonal multi-shell-type (PMS-type) Cu NWs.

2. Simulation procedures

To describe multi-shell-type NWs, we use the notation n–n'–n''–n''' introduced by Kondo and Takayanagi [1, 22], when the NW consists of coaxial tubes with n, n', n'', n''' helical atom rows ($n > n' > n'' > n'''$). The initial atomic arrangement in the wire was relaxed by the steepest-descent (SD) method. This MD simulation used the same MD methods as our previous work [39–41], with a time step of 0.5 fs. The MD code used the velocity Verlet algorithm, a Gunstern–Berendsen thermostat to maintain constant temperature, a periodic boundary condition along the wire axis, and neighbour lists to improve computing performance [42]. For Cu, we have used a many-body potential function of the second-moment approximation of a tight-binding scheme [43] that has already been tested on nanoclusters [40, 44, 45] and NWs [7, 8, 14, 39, 46].

3. Results and discussion

In this investigation, we used the PMS-type Cu NWs obtained by the extension of decahedron model particles. The length of the supercell for the PMS-type Cu NWs is 63.284 Å. Figures 1(*a*)–(*c*) show PMS-type Cu NWs with diameters of 8, 11.5, and 15 Å, respectively. As the diameter of the pentagonal NW increases, a hexagonal lattice that is split from the core pentagon appears. Figure 1(*d*) shows the spreading sheets of the PMS-type Cu NW shown in figure 1(*a*). Each sheet is composed of a square network in a $\{100\}$ facet of fcc, excluding the central atomic strands. The wire axis of the PMS-type Cu NWs is always along the $\langle 110 \rangle$ direction. Considering the fact that shells in the cylindrical multi-shell-type (CMS-type) NWs are composed by circular folding of the triangular network in a $\{111\}$ facet of fcc, it is interesting that shells in the PMS-type NWs are composed by pentagonal folding of a square network. Furthermore, subunits of the PMS-type NWs divided by five triangles show stacking sequences oriented in the $\langle 100 \rangle$ direction. These look like quadrangular pyramids, as shown in figure 1(*e*), which shows the subunit indicated by a triangle in figure 1(*c*). The distance of the nearest-neighbouring atoms, 2.556 Å, is very slightly smaller than that of the fcc bulk material. Previous experimental results for Au nanobridges [20] can help to explain the structural properties of the PMS-type NWs. Kondo and Takayanagi [20] have shown that a straight, uniform nanobridge with the $\{111\}$ planes along the $\langle 110 \rangle$ wire axis is stabilized, and the electron diffraction pattern of the nanobridge includes both square and hexagonal lattices.

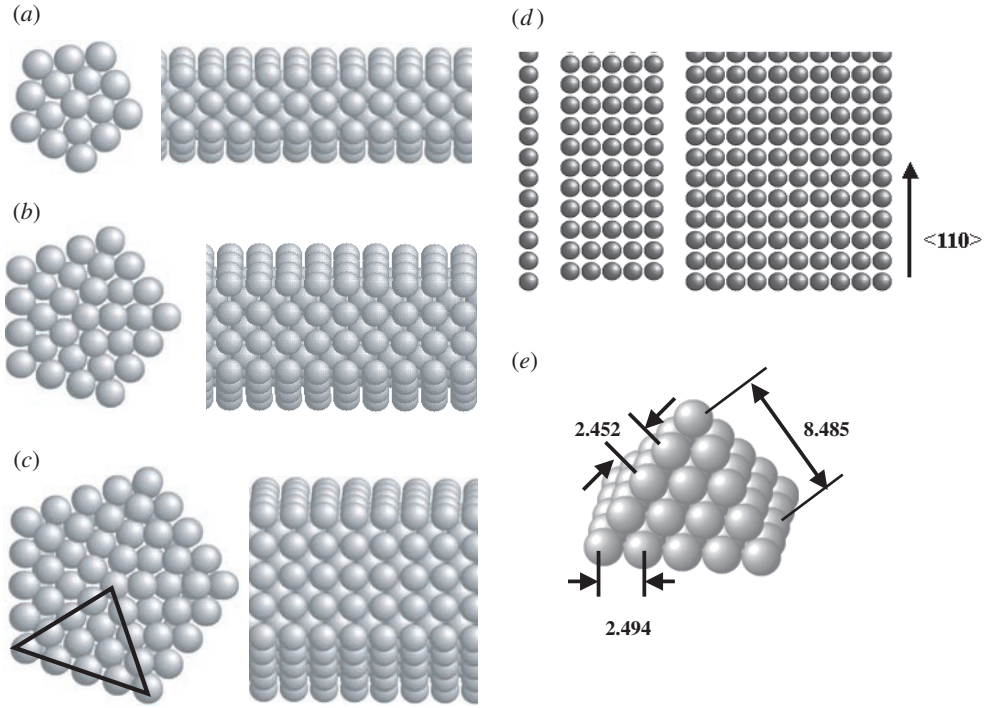

Figure 1. PMS-type Cu NWs. (*a*) 10–5–1, (*b*) 15–10–5–1, and (*c*) 20–15–10–5–1. (*d*) The spreading sheets of (*a*). (*e*) The subunit indicated by a triangle in (*c*): a quadrangular pyramid oriented in the ⟨100⟩ direction. The unit is Å.

They proposed a hexagonal prism model for the nanobridge, where the surface layers have hexagonal close-packed (HCP) lattices, and the core has an fcc structure. Since PMS-type NWs are composed of a central atomic strand and pentagonal tubes made by folding {100} sheets five times, and their subunits have a quadrangular-pyramid shape, the electron diffraction pattern of the pentagonal NWs shows both square and hexagonal lattices [24]. For PMS-type NWs, the surface has an fcc structure, and the core has a hexagonal structure split from the core pentagon.

The lattice constant of CMS-type Cu NWs in the direction of the wire axis was found to be 2.121 Å. For CMS-type 16–11–6–1 Cu NWs, the distances from the wire centre to the atomic position in each shell are 6.494, 4.419, and 2.374 Å, and the cohesive energies per atom of each shell are −3.030, −3.450, −3.465, and −3.386 eV, compared with −3.544 eV for the bulk material. For PMS-type 20–15–10–5–1 Cu NWs, the lattice constant in the direction of the wire axis is 2.462 Å. Distances from the wire centre to atomic positions at the vertices of each pentagonal shell are 8.485, 6.345, 4.230, and 2.113 Å, and the average cohesive energies per atom of each shell are −2.994, −3.441, −3.485, −3.476, and −3.425 eV. In the present study, the average energies per atom (total cohesive energy per total atom number) for the CMS-type 16–11–6–1 and the PMS-type 20–15–10–5–1 NWs are −3.253 and −3.277 eV, respectively.

We also investigated the correlation functions for PMS-type Cu NWs, to investigate the structural properties. Figure 2 shows the angular correlation function (ACF), and the pair correlation function (PCF) of PMS-type Cu NWs at 0 and 300 K. These are compared with

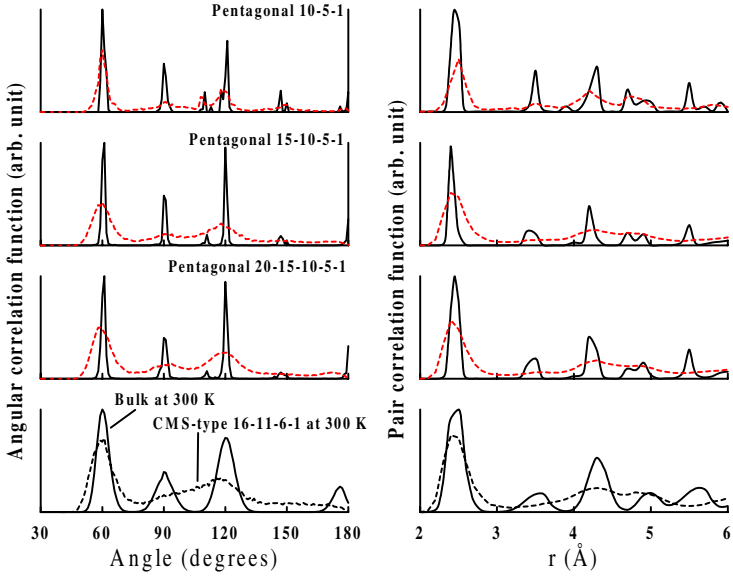

Figure 2. The ACF and PCF (see the text) of the PMS-type Cu NWs at both 0 and 300 K, compared with those of CMS-type 16–11–6–1 Cu NW and fcc bulk material at 300 K. The solid and dashed curves indicate temperatures of 0 and 300 K, respectively.

those of CMS-type 16–11–6–1 Cu NW and the fcc bulk material, at 300 K. The solid and the dashed curves indicate the ACFs and PCFs at 0 and 300 K, respectively. For the ACFs and PCFs at 0 K, the main peaks of the PMS-type Cu NWs are in good agreement with those of the fcc bulk Cu. The ACFs and PCFs of the CMS-type Cu NWs are different from those of the bulk Cu in this work, as well as in the previous work [7–9]. In the calculation of the ACFs, because we considered the first-nearest-neighbouring atoms, the small peaks related to the pentagonal structures appear at about 108° and 144°. However, at room temperature, the ACFs and the PCFs of the PMS-type Cu NWs tend to those of CMS-type Cu NWs. This means that the original Cu NW of figure 1(*a*) changed the PMS-type NWs to CMS-type NWs at 300 K. Figure 3(*a*) shows the structure obtained by MD simulation of the Cu NW of figure 1(*a*) at 300 K. The surface structures of this NW are composed of both square and hexagonal lattices, and the region of the hexagonal lattice is greater than that of the other. The labels A and C in figure 3(*a*) indicate pentagon rings, and the label B in figure 3(*a*) indicates a decagon ring that is nearly a circle; each ring is also represented with its cell. The 10–5–1 Cu NW formed by circular folding of {111} sheets has a CMS-type structure composed of cells labelled A, B, and C, and its cell sequence is A–B–C–B along the wire axis. This structural property can be explained by the property shown in the nanocluster series obtained from expansion of dodecahedron model particles. Figure 4 shows the stable nanoclusters related to the dodecahedron model with the 12–6–1 hexagonal multi-shell. The labels A and C in figure 4 indicate rings, and the label B in figure 4 indicates a dodecagonal ring that is nearly a circle. As the outer ring with 12 atoms is added along the axis direction, the outer ring follows the sequence A–B–C–B, and the wire becomes CMS-type NW with a {111}-like surface. When the number of the outer rings with 12 atoms is two, they are composed of just A and C. The properties of decahedron model particle series are the same as those of the dodecahedron model particle. We can see that the ultrathin PMS-type Cu NWs have structures composed of an outer ring sequence A–B–C–B.

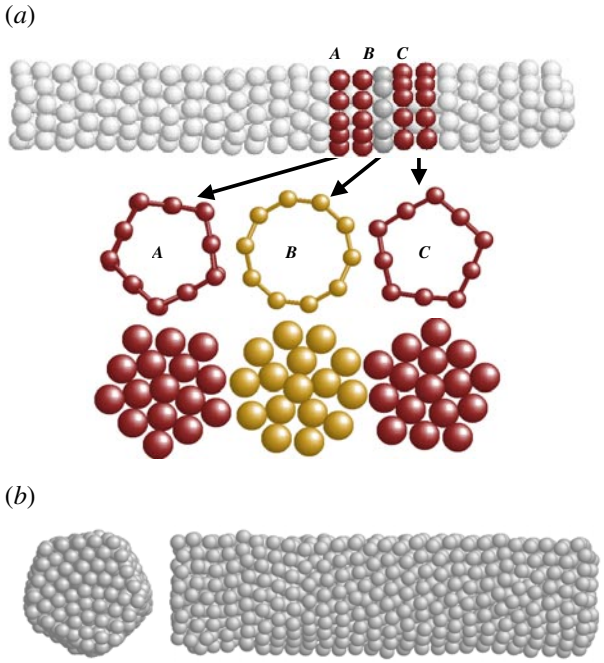

Figure 3. (*a*) The structure obtained by MD simulation at 300 K for the cases of figure 1(*a*). The labels A and C indicate the pentagonal rings and the label B indicates a decagonal ring that is nearly a circle. Each ring is also represented with its cell. (*b*) The structure obtained by MD simulation at 300 K in the cases of figure 1(*c*).

From the above results and discussion, we can expect that, at room temperature, ultrathin PMS-type 10–5–1 Cu NWs with {100} surfaces will seldom be found, but ultrathin CMS-type 10–5–1 NWs with {111}-like surfaces will often be found. This is in good agreement with the results that ultrathin Au NWs are CMS-type structures. In the case of PMS-type 15–10–5–1 Cu NW, similar results are achieved. However, in figure 3(*b*), the PMS-type 20–15–10–5–1 Cu NW maintains the pentagonal structure, although hexagonal surfaces appear in some regions. We can see that as the diameter increases, the probability that PMS-type Cu NWs maintain their structures increases. The diameters of self-assembled pentagonal Cu nanorods are above 10 nm [24]. Therefore, we simulated the PMS-type Cu NW with a diameter of about 33 Å. Figures 5(*a*) and (*b*) show the structures after MD simulations at 100 ps, with PMS-type 40–35–30–25–20–15–10–5–1 NWs made at 300 K from pentagonal tubes with {100} surfaces, and with decagonal multi-shell 46–41–36–31–26–21–16–11–6–1 NWs made by circular folding of {111} facets. The larger diameter PMS-type Cu NW is not transformed into CMS-type Cu NW, as shown in figure 5(*a*), but maintains a pentagonal structure with a square lattice on the surface. In the case of the decagonal multi-shell Cu NW with a diameter of 37 Å, five hexagonal lattice regions and five square lattice regions make up its cross-section, and alternately appear in turning on the axis. The ACFs and PCFs of figures 5(*a*) and (*b*) are similar to those of the bulk material, as shown in figure 5(*c*). Polygonal multi-shell-type Cu NWs with diameters of several nanometres can be found in the stable structures.

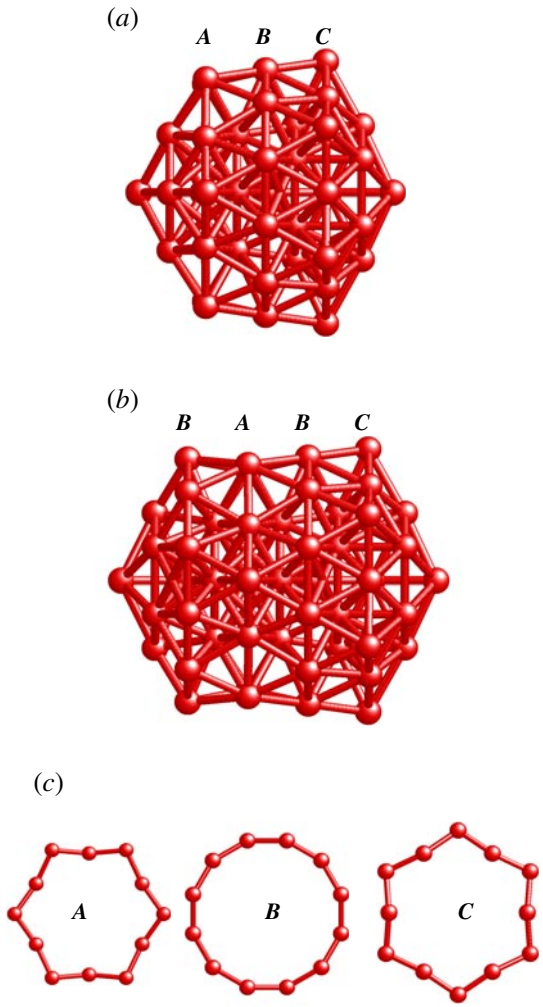

Figure 4. The stable nanoclusters related to the dodecahedron model with the 12–6–1 hexagonal multi-shell. The labels A and C indicate the hexagonal rings and the label B indicates the dodecagonal ring that is nearly a circle.

4. Conclusions

In this investigation, we have revealed the structures and properties of PMS-type Cu NWs, which are each composed of a central atomic strand and pentagonal tubes made by folding $\{100\}$ sheets five times. While the structural properties of CMS-type NWs do not conform to an fcc structure [7–9], the structural properties of PMS-type Cu NWs are close to those of an fcc structure, as the subunits each have a quadrangular-pyramid shape oriented in the $\langle 100 \rangle$ direction. This simulation showed that, at room temperature, ultrathin pentagonal Cu NWs whose diameters are one nanometre more or less are not found, but PMS-type Cu NWs with diameters of several nanometres are found in the stable structures. From these results we anticipate applications of pentagonal Cu NWs with diameters of several nanometres in nanoelectronic devices.

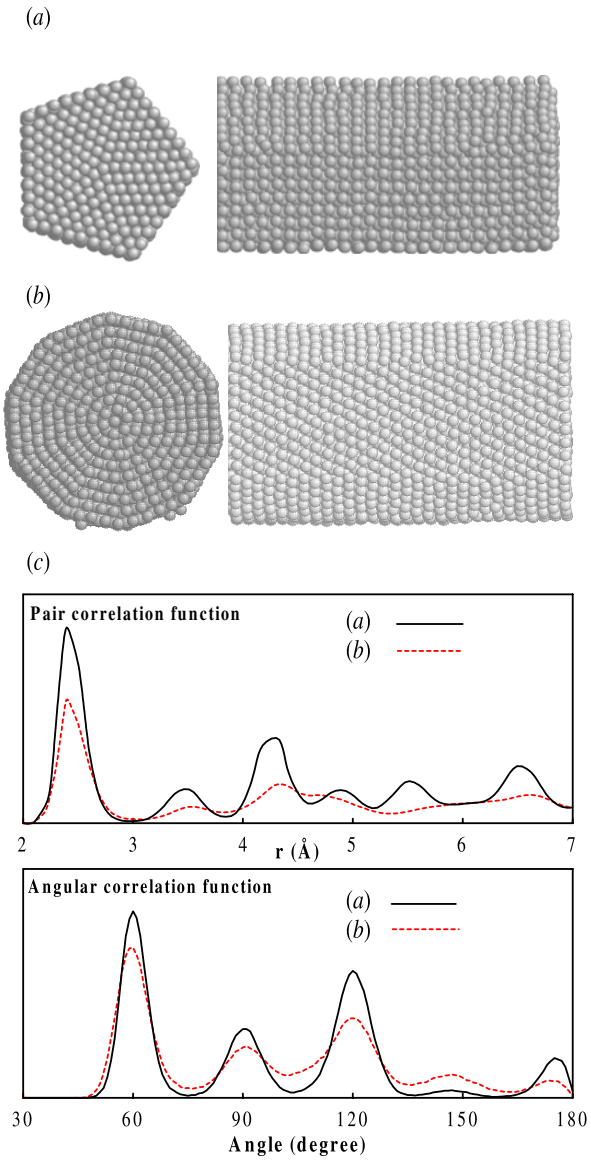

Figure 5. (*a*) PMS-type 40–35–30–25–20–15–10–5–1 Cu NW at 300 K. (*b*) The decagonal structure 46–41–36–31–26–21–16–11–6–1 Cu NW at 300 K. (*c*) The PCF and the ACF of (*a*) and (*b*).

As real Cu NWs that exist outside of a vacuum chamber would be covered with other materials, such as surfactant ligands and bio-organic films, we will extend this study to include the effects of ligands and the stability of Cu NWs.

References

[1] Wang B, Yin S, Wang G, Buldum B and Zhao J 2001 *Phys. Rev. Lett.* **86** 2046
[2] Bilalbegovic G 1998 *Phys. Rev.* B **58** 15 412
[3] Tosatti E, Prestipino S, Kostlmeier S, Dal Corso A and Di Tolla F D 2001 *Science* **291** 288

[4] Bilalbegovic G 2000 *Solid State Commun.* **115** 73
[5] Torres J A, Tosatti E, Dal Corso A, Ercolessi F, Kohanoff J J, Di Tolla F D and Soler J M 1999 *Surf. Sci.* **426** L441
[6] Bilalbegovic G 2000 *Comput. Mater. Sci.* **18** 333
[7] Hwang H J and Kang J W 2002 *J. Korean Phys. Soc.* **40** 283
[8] Kang J W and Hwang H J 2002 *Mol. Simul.* at press
[9] Kang J W and Hwang H J 2002 *Phys. Rev.* B *Preprint* cond-mat0202032
[10] Gülseren O, Erolessi F and Tosatti E 1998 *Phys. Rev. Lett.* **80** 3775
[11] Di Tolla F, Dal Corso A, Torres J A and Tosatti E 2000 *Surf. Sci.* **456** 947
[12] Gülseren O, Erolessi F and Tosatti E 1995 *Phys. Rev.* B **51** 7377
[13] Finbow G M, Lynden-Bell R M and McDonald I R 1997 *Mol. Phys.* **92** 705
[14] Wang B, Yin S, Wang G and Zhao J 2001 *J. Phys.: Condens. Matter* **13** L403
[15] Yanson A I, Yanson I K and van Ruitenbeek J M 2000 *Phys. Rev. Lett.* **84** 5832
[16] Puska M J, Ogando E and Zabala N 2001 *Phys. Rev.* B **64** 033401
[17] Tenne R, Margulis L, Genut M and Hodes G 1992 *Nature* **360** 444
[18] Margulis L, Salitra G, Tenne R and Tallenker M 1993 *Nature* **365** 113
[19] Hacohen Y R, Grunbaum E, Tenne R and Tallenker M 1998 *Nature* **395** 336
[20] Kondo Y and Takayanagi K 1997 *Phys. Rev. Lett.* **79** 3455
[21] Ohnishi H, Kondo Y and Takayanagi K 1998 *Nature* **395** 780
[22] Kondo Y and Takayanagi K 2000 *Science* **289** 606
[23] Rodrigues V, Fuhrer T and Ugarte D 2000 *Phys. Rev. Lett.* **85** 4124
[24] Lisiecki I, Filankembo A, Sack-Kongehl H, Weiss K, Pileni M-P and Urban J 2000 *Phys. Rev.* B **61** 4968
[25] Yun W S *et al* 2000 *J. Vac. Sci. Technol.* A **18** 1329
[26] Kang J W and Hwang H J 2002 *J. Korean Phys. Soc. Preprint* cond-mat0202033
[27] Michaelian K, Rendon N and Garzon I L 1999 *Phys. Rev.* B **60** 2000
[28] Erkoc S 2000 *Physica* E **8** 210
[29] Li T X, Yin S Y, Ji Y L, Wang B L, Wang G H and Zhao J J 2000 *Phys. Lett.* A **267** 403
[30] Catlow C R A, Bulatov V L and Grimes R W 1997 *Nucl. Instrum. Methods Phys. Res.* B **122** 301
[31] Rongwu L, Zhengying P and Yukun H 1996 *Phys. Rev.* B **53** 4156
[32] Lammers U and Borstel G 1994 *Phys. Rev.* B **49** 17 360
[33] Landman U 1998 *Solid State Commun.* **107** 693
[34] Whetten R L, Khoury J T, Alvarez M M, Murthy S, Vezmar I, Wang Z L, Stephens P W, Cleveland C L, Luedtke W D and Landman U 1996 *Adv. Mater.* **8** 428
[35] Cleveland C L, Landman U, Shafigullin M N, Stephens P W and Whetten R L 1997 *Z. Phys.* D **40** 503
[36] Cleveland C L, Landman U, Schaaff T G, Shafigullin M N, Stephens P W and Whetten R L 1997 *Phys. Rev. Lett.* **79** 1873
[37] Schaaff T G, Shafigullin M N, Khoury J T, Vezmar I, Whetten R L, Cullen W G, First P N, Gutierrez-Wing C, Ascensio M J and Jose-Yacaman M J 1997 *J. Phys. Chem.* B **101** 7885
[38] Alvarez M M, Khoury J T, Schaaff T G, Shafigullin W, Vezmar I and Whetten R L 1997 *Chem. Phys. Lett.* **266** 91
[39] Kang J W and Hwang H J 2001 *J. Korean Phys. Soc.* **38** 695
[40] Kang J W and Hwang H J 2001 *Phys. Rev.* B **64** 014108
[41] Kang J W, Choi K S, Byun K R and Hwang H J 2000 *J. Korean Phys. Soc.* **36** 248
Kang J W, Choi K S, Byun K R and Hwang H J 2001 *J. Vac. Sci. Technol.* A **19** 1902
Kang J W, Choi K S, Kang J C and Hwang H J 2001 *J. Korean Phys. Soc.* **38** 158
Kang J W and Hwang H J 2001 *Comput. Mater. Sci.* **21** 509
[42] Allen M P and Tildesley D J 1987 *Computer Simulation of Liquids* (Oxford: Clarendon) ch 4
[43] Cleri F and Rosato V 1993 *Phys. Rev.* B **48** 22
[44] Palacios F J, Iniguez M P, Lopez M J and Alonso J A 1999 *Phys. Rev.* B **60** 2908
[45] Li T X, Yin S Y, Ji Y L, Wang B L, Wang G H and Zhao J J 2000 *Phys. Lett.* A **267** 403
[46] Kang J W and Hwang H J 2001 *Nanotechnology* **12** 295